Supporting Information

Bandgap-engineered nitrogen plasma functionalized biochar-TiO_2 composite for enhanced antibiotic photodegradation

Rayhan Bin Masud[1,¥], Samiha Raisa Alam[1,¥], Hridoy Roy[1,2,¥,#], Mohammad Jellur Rahman[3] and Md. Shahinoor Islam[1,4]*

[1]*Department of Chemical Engineering, Bangladesh University of Engineering and Technology, Dhaka 1000, Bangladesh*

[2]*Department of Chemical Engineering, University of Michigan, Ann Arbor, Michigan 48109, United States*

[3]*Department of Physics, Bangladesh University of Engineering and Technology, Dhaka 1000, Bangladesh*

[4]*Department of Textile Engineering, Daffodil International University, Dhaka 1341, Bangladesh*

Table S1: Macroscopic color characteristics and visual appearance of synthesized photocatalysts(a) Pure TiO_2, (b) Biochar-supported TiO_2 (BC–TiO_2), (c) N-doped Biochar–TiO_2 after AC-plasma treatment (Plasma BC–TiO_2).

SL. No.	Catalyst	Description of catalysts	Visual appearance
1	TiO_2	Pure Anatase TiO_2	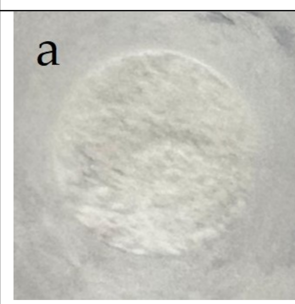

2	BC-TiO_2	Biochar-supported TiO_2	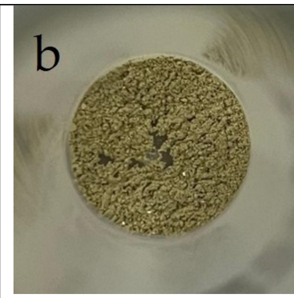
3	Plasma BC-TiO_2	AC-Plasma treated N-Doped Biochar-supported TiO_2	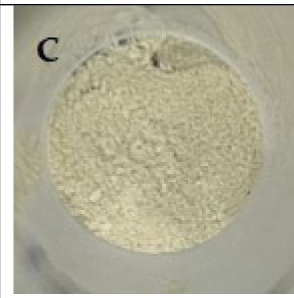

S1. Kinetic Model Justification

The Langmuir-Hinshelwood (L-H) equation (Equation 3), a first-order differential equation, was solved using the Perturbation-Iteration Algorithms (PIA) [1]. Using the PIA method, an approximate solution to Equation 3 can be obtained as an exponential function of time:

$$C = C_0 e^{-kKt}\left(1 + C_0 K\left(1 - e^{-kKt}\right)\right) \quad \text{(S1)}$$

MATLAB program was used to determine the reaction rate constant k and the adsorption equilibrium coefficient K, and validate the application of the L-H Model in this experiment. Table S2 demonstrates the comparison between the L-H model, simplified pseudo-first-order kinetics, and zero-order kinetics.

Table S2: Comparative analysis between L-H model, Pseudo-first-order, and Zero-order kinetics

Catalyst	Initial CIP Concentration (ppm)	L-H Model				Pseudo-first-order kinetics		Zero-order kinetics		
		K $(min)^{-1}$	k $(min)^{-1}$	k_{app} (K*k) $(min)^{-1}$	R^2	k_{app} $(min)^{-1}$	R^2	k_{app} ppm $(min)^{-1}$	k_{app} $(min)^{-1}$	R^2
TiO_2	10	0.0003	6.60	0.0023	0.96	0.0022	0.96	0.02	0.002	0.90
	30	0.0003	20.67	0.0062	0.86	0.0022	0.94	0.05	0.0016	0.91
	50	0.0004	3.75	0.0015	0.566	0.0009	0.86	0.023	0.0046	0.86
BC-TiO_2	10	0.001	6.1	0.0061	0.93	0.0068	0.87	0.03	0.003	0.74
	30	0.0013	3.31	0.0043	0.96	0.0034	0.95	0.06	0.002	0.91
	50	0.0015	1.87	0.0028	0.64	0.00126	0.88	0.048	0.0096	0.86
Plasma BC-TiO_2	10	0.00098	22.35	0.0219	0.99	0.0196	0.99	0.06	0.006	0.94
	30	0.00098	13.88	0.0136	0.99	0.011	0.99	0.15	0.005	0.94
	50	0.0012	45	0.054	0.89	0.048	0.96	0.16	0.0032	0.94

At low concentration (10 ppm), high linearity ($R^2 \geq 0.93$–0.99) and close agreement between L–H and pseudo-first-order k_{app} values confirm the dilute-limit condition ($KC \ll 1$), under which the L–

H rate expression mathematically reduces to apparent first-order kinetics [2]. With increasing concentration (30–50 ppm), the declining R^2 values for the L-H model and the comparable or higher zero-order fits, indicate progressive surface saturation and transition to photon- or surface-limited regimes at high surface coverage [3]. Notably, this deviation reflects physically meaningful regime transitions rather than model inadequacy, as zero-order behavior is theoretically expected once active sites are saturated, and reaction rates become independent of bulk concentration [4]. Moreover, plasma BC–TiO_2 exhibited consistently high L–H conformity across all concentrations ($R^2 \geq 0.89$) with stable K and k values, confirming maintenance of adsorption–desorption equilibrium and surface reaction controlled kinetics due to plasma induced functionalization and defect formation, as reported for plasma-treated N_2–TiO_2 systems in recent studies[5,6] . Collectively, the inclusion of full L–H parameters and their systematic variation with concentration and catalyst composition provides a physically justified basis for the chosen kinetic framework.

S2. MATLAB Code for L-H Model

MATLAB code for finding L-H parameters (10 ppm CIP for Plasma BC-TiO_2) and C vs t graph using Equation S1 is given below:

```
% Experimental data
t = [0 30 50 75 100 140]';
C = [10 7.74076 5.37263 3.56818 2.14308 0.88736]';
C0 = 10;   % Initial concentration (fixed)
% Langmuir–Hinshelwood kinetic model
model = @(p,t) C0.*exp(-p(1).*p(2).*t) .* ...
            (1 + C0.*p(2).*(1 - exp(-p(1).*p(2).*t)));
% Initial guess [kr, K]
```

```
p0 = [0.00001 0.00001];

% Lower bounds

lb = [0 0];

% Nonlinear least squares fit

opts = optimoptions('lsqcurvefit','Display','off');

[p,resnorm,residual,exitflag,output] = ...

    lsqcurvefit(model,p0,t,C,lb,[],opts);

% Extract parameters

kr = p(1);

K  = p(2);

k_app = kr*K;

% Model prediction at experimental points

C_fit = model(p,t);

% ---- R^2 calculation ----

SS_res = sum((C - C_fit).^2);          % residual sum of squares

SS_tot = sum((C - mean(C)).^2);        % total sum of squares

R2 = 1 - SS_res/SS_tot;

% Display results

fprintf('kr     = %.4f\n', kr);

fprintf('K      = %.4f\n', K);

fprintf('k_app  = %.4f min^-1\n', k_app);

fprintf('R^2    = %.4f\n', R2);
```

The same code was used for determining parameters for the respective samples and CIP values.

S3. Control Experiment

Control experiment was conducted using UV light (254 nm), without adding any photocatalysts. The results are depicted as follows:

Table S3a: Control experiment for 10 ppm Ciprofloxacin

Time (min)	CIP Remaining (ppm)	Degradation (%)
0	10.00	0.0
20	9.85	1.5
45	9.72	2.8
70	9.60	4.0
110	9.52	4.8

Table S3b: Control experiment for 30 ppm Ciprofloxacin

Time (min)	CIP Remaining (ppm)	Degradation (%)
0	30.00	0.0
20	29.60	1.3
45	29.30	2.3
70	29.05	3.2
110	28.70	4.3

Table S3c: Control experiment for 50 ppm Ciprofloxacin

Time (min)	CIP Remaining (ppm)	Degradation (%)
0	50.00	0.0
20	49.40	1.2
45	49.10	1.8
70	48.75	2.5
110	48.30	3.4

References

1. Analysis of Langmuir-Hinshelwood Kinetics Model for Photocatalytic Degradation of Aqueous Direct Blue 71 Through Analytical Expression | Semantic Scholar. Accessed January 15, 2026. https://www.semanticscholar.org/paper/Analysis-of-Langmuir-Hinshelwood-Kinetics-

Model-for-Loghambal-
Catherine/fa3cba3b4b66cb35fa7895e9beaf110489fa0fef?utm_source=direct_link

2. Turchi CS, Ollis DF. Photocatalytic degradation of organic water contaminants: Mechanisms involving hydroxyl radical attack. *Journal of Catalysis*. 1990;122(1):178-192. doi:10.1016/0021-9517(90)90269-P

3. Photocatalytic degradation of ciprofloxacin from water with waste polystyrene and TiO2 composites: Heliyon. Accessed January 15, 2026. https://www.cell.com/heliyon/fulltext/S2405-8440(24)01464-6?_returnURL=https%3A%2F%2Flinkinghub.elsevier.com%2Fretrieve%2Fpii%2FS2405844024014646%3Fshowall%3Dtrue

4. Pera-Titus M, García-Molina V, Baños MA, Giménez J, Esplugas S. Degradation of chlorophenols by means of advanced oxidation processes: a general review. *Applied Catalysis B: Environmental*. 2004;47(4):219-256. doi:10.1016/j.apcatb.2003.09.010

5. Liu X, Hua R, Niu J, Zhang Z, Zhang J. N2 plasma treatment TiO2 nanosheets for enhanced visible light-driven photocatalysis. *Journal of Alloys and Compounds*. 2021;881:160509. doi:10.1016/j.jallcom.2021.160509

6. Hosseini S, Amoozadeh A. Plasma Treatment as a Promising Environmentally Benign Approach for Synthesis of Valuable Multi-gas Doped Nano-TiO2-P25: An Efficient Way to Boost the Photocatalytic Performance under Visible Light Illumination. *Photochemistry and Photobiology*. 2021;97(4):672-687. doi:10.1111/php.13374